Universality and Superscaling in Lepton-Nucleus Scattering

Maria Barbaro
Dipartimento di Fisica and INFN, Torino, Italy

INT Workshop
Theoretical Developments in Neutrino-Nucleus Scattering
December 5-9, 2016, Seattle

Collaboration: J. Amaro, J. Caballero, A. De Pace, B. Donnelly,
R. Gonzalez, M. Ivanov, G. Megias, I. Ruiz Simo

Contents

Contents

Connection between neutrino- and electron- scattering

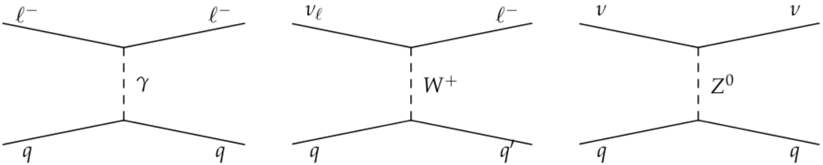

(a) Electromagnetic scattering (b) Charged-current scattering (c) Neutral-current scattering

- Electron-nucleus interaction, mediated by γ (EM) and Z^0 (weak)
- Neutrino-nucleus interaction, mediated by $W^\pm$ (CC) and Z^0 (NC)

Connection between neutrino- and electron- scattering

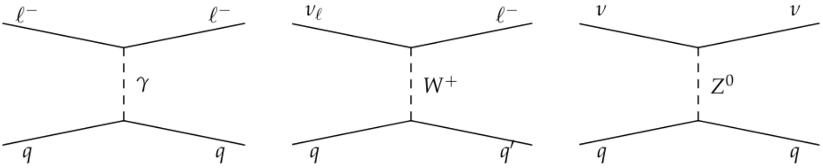

(a) Electromagnetic scattering (b) Charged-current scattering (c) Neutral-current scattering

- Electron-nucleus interaction, mediated by γ (EM) and Z^0 (weak)
- Neutrino-nucleus interaction, mediated by $W^\pm$ (CC) and Z^0 (NC)
- Neutrinos can probe both the vector and axial nuclear responses, unlike (unpolarized) electrons, which are (essentially) sensitive only to the vector response.

Connection between neutrino- and electron- scattering

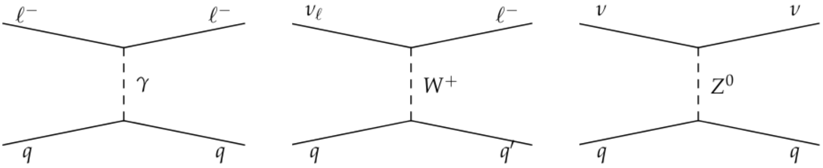

(a) Electromagnetic scattering (b) Charged-current scattering (c) Neutral-current scattering

- Electron-nucleus interaction, mediated by γ (EM) and Z^0 (weak)
- Neutrino-nucleus interaction, mediated by $W^\pm$ (CC) and Z^0 (NC)
- Neutrinos can probe both the vector and axial nuclear responses, unlike (unpolarized) electrons, which are (essentially) sensitive only to the vector response.
- Many high quality $e - A$ data exist, which must be used to test models, and can also can be used as an input for predicting $\nu - A$ observables.

Connection between neutrino- and electron- scattering

- The experimental conditions are different:

Connection between neutrino- and electron- scattering

- The experimental conditions are different:
  - (e, e'): the electron energy is well determined and different mechanisms can be clearly identified by knowing the energy and momentum transfer (e.g., QE scattering corresponds to a well-defined peak in the ω spectrum).

Connection between neutrino- and electron- scattering

- The experimental conditions are different:
  - (e, e'): the electron energy is well determined and different mechanisms can be clearly identified by knowing the energy and momentum transfer (e.g., QE scattering corresponds to a well-defined peak in the ω spectrum).
  - CC (ν_l, l): E_ν is broadly distributed in the neutrino beam and different mechanisms can contribute to the same kinematics of the outgoing lepton (e.g., QE is defined as "no pions in the final state").

Connection between neutrino- and electron- scattering

- The experimental conditions are different:
  - (e, e'): the electron energy is well determined and different mechanisms can be clearly identified by knowing the energy and momentum transfer (e.g., QE scattering corresponds to a well-defined peak in the ω spectrum).
  - CC (ν_l, l): E_ν is broadly distributed in the neutrino beam and different mechanisms can contribute to the same kinematics of the outgoing lepton (e.g., QE is defined as "no pions in the final state").
  - NC $(\nu_l, \nu_l')N$: the final neutrino cannot be detected, the ejected nucleon is observed (u-channel scattering). In this case the energy transfer is not fixed, even for monochromatic neutrino beams.

Connection between neutrino- and electron- scattering

- The experimental conditions are different:
  - (e, e'): the electron energy is well determined and different mechanisms can be clearly identified by knowing the energy and momentum transfer (e.g., QE scattering corresponds to a well-defined peak in the ω spectrum).
  - CC (ν_l, l): E_ν is broadly distributed in the neutrino beam and different mechanisms can contribute to the same kinematics of the outgoing lepton (e.g., QE is defined as "no pions in the final state").
  - NC $(\nu_l, \nu_l')N$: the final neutrino cannot be detected, the ejected nucleon is observed (u-channel scattering). In this case the energy transfer is not fixed, even for monochromatic neutrino beams.
- The **SuperScaling** approach exploits universal features of lepton-nucleus scattering to connect the two processes.

Connection between neutrino- and electron- scattering

- The experimental conditions are different:
  - (e, e'): the electron energy is well determined and different mechanisms can be clearly identified by knowing the energy and momentum transfer (e.g., QE scattering corresponds to a well-defined peak in the ω spectrum).
  - CC (ν_l, l): E_ν is broadly distributed in the neutrino beam and different mechanisms can contribute to the same kinematics of the outgoing lepton (e.g., QE is defined as "no pions in the final state").
  - NC $(\nu_l, \nu_l')N$: the final neutrino cannot be detected, the ejected nucleon is observed (u-channel scattering). In this case the energy transfer is not fixed, even for monochromatic neutrino beams.
- The **SuperScaling** approach exploits universal features of lepton-nucleus scattering to connect the two processes.
- **"Superscaling" is the simultaneous occurrence of scaling of first and second kinds**
  - Day *et al.*, Annu. Rev. Nucl. Part. Sci. (1990)
  - Donnelly and Sick, PRL82 & PRC60 (1999)

Definitions

Definitions

- Inclusive electromagnetic reduced cross section $F(q, \omega) \equiv \frac{d^2\sigma/d\omega d\Omega}{\sigma_M(v_L G_L + v_T G_T)}$
  $d^2\sigma/d\omega d\Omega = \sigma_{Mott}\,(v_L R_L + v_T R_T)$
  $R_{L,T}(q, \omega)$ Longitudinal and Transverse nuclear response functions
  $G_{L,T}(q, \omega)$ elementary functions depending on the nucleonic form factors
  $v_{L,T}(q, \omega, \theta)$ kinematical factors

Definitions

- Inclusive electromagnetic reduced cross section $F(q,\omega) \equiv \frac{d^2\sigma/d\omega d\Omega}{\sigma_M(v_L G_L + v_T G_T)}$
  $d^2\sigma/d\omega d\Omega = \sigma_{Mott}\,(v_L R_L + v_T R_T)$
  $R_{L,T}(q,\omega)$ Longitudinal and Transverse nuclear response functions
  $G_{L,T}(q,\omega)$ elementary functions depending on the nucleonic form factors
  $v_{L,T}(q,\omega,\theta)$ kinematical factors
- If F becomes function of only one variable, scaling of first kind occurs

Definitions

- Inclusive electromagnetic reduced cross section $F(q,\omega) \equiv \frac{d^2\sigma/d\omega d\Omega}{\sigma_M(v_L G_L + v_T G_T)}$
  $d^2\sigma/d\omega d\Omega = \sigma_{Mott}\,(v_L R_L + v_T R_T)$
  $R_{L,T}(q,\omega)$ Longitudinal and Transverse nuclear response functions
  $G_{L,T}(q,\omega)$ elementary functions depending on the nucleonic form factors
  $v_{L,T}(q,\omega,\theta)$ kinematical factors
- If F becomes function of only one variable, scaling of first kind occurs
- This variable, a combination of q and ω, is called scaling variable
  - $y(q,\omega) \to$ minimum missing momentum
  - $\psi(q,\omega;k_F) \to$ minimum kinetic energy of the initial nucleon divided by the Fermi kinetic energy (dimensionless)
  - $\psi \simeq y/k_F$
  - the QEP occurs at $\psi = y = 0$

Definitions

- Inclusive electromagnetic reduced cross section $F(q,\omega) \equiv \frac{d^2\sigma/d\omega d\Omega}{\sigma_M(v_L G_L + v_T G_T)}$
  $d^2\sigma/d\omega d\Omega = \sigma_{Mott}\,(v_L R_L + v_T R_T)$
  $R_{L,T}(q,\omega)$ Longitudinal and Transverse nuclear response functions
  $G_{L,T}(q,\omega)$ elementary functions depending on the nucleonic form factors
  $v_{L,T}(q,\omega,\theta)$ kinematical factors
- If F becomes function of only one variable, scaling of first kind occurs
- This variable, a combination of q and ω, is called scaling variable
  - $y(q,\omega) \rightarrow$ minimum missing momentum
  - $\psi(q,\omega;k_F) \rightarrow$ minimum kinetic energy of the initial nucleon divided by the Fermi kinetic energy (dimensionless)
  - $\psi \simeq y/k_F$
  - the QEP occurs at $\psi = y = 0$
- $F(\psi)$ is called the scaling function

Definitions

- Inclusive electromagnetic reduced cross section $F(q,\omega) \equiv \frac{d^2\sigma/d\omega d\Omega}{\sigma_M(v_L G_L + v_T G_T)}$
  $d^2\sigma/d\omega d\Omega = \sigma_{Mott}\,(v_L R_L + v_T R_T)$
  $R_{L,T}(q,\omega)$ Longitudinal and Transverse nuclear response functions
  $G_{L,T}(q,\omega)$ elementary functions depending on the nucleonic form factors
  $v_{L,T}(q,\omega,\theta)$ kinematical factors
- If F becomes function of only one variable, scaling of first kind occurs
- This variable, a combination of q and ω, is called scaling variable
  - $y(q,\omega) \rightarrow$ minimum missing momentum
  - $\psi(q,\omega;k_F) \rightarrow$ minimum kinetic energy of the initial nucleon divided by the Fermi kinetic energy (dimensionless)
  - $\psi \simeq y/k_F$
  - the QEP occurs at $\psi = y = 0$
- $F(\psi)$ is called the scaling function
- $f(\psi) \equiv k_F \times F(\psi)$ super-scaling function.

Definitions

- Inclusive electromagnetic reduced cross section $F(q,\omega) \equiv \frac{d^2\sigma/d\omega d\Omega}{\sigma_M(v_L G_L + v_T G_T)}$
  $d^2\sigma/d\omega d\Omega = \sigma_{Mott}\,(v_L R_L + v_T R_T)$
  $R_{L,T}(q,\omega)$ Longitudinal and Transverse nuclear response functions
  $G_{L,T}(q,\omega)$ elementary functions depending on the nucleonic form factors
  $v_{L,T}(q,\omega,\theta)$ kinematical factors
- If F becomes function of only one variable, scaling of first kind occurs
- This variable, a combination of q and ω, is called scaling variable
  - $y(q,\omega) \rightarrow$ minimum missing momentum
  - $\psi(q,\omega;k_F) \rightarrow$ minimum kinetic energy of the initial nucleon divided by the Fermi kinetic energy (dimensionless)
  - $\psi \simeq y/k_F$
  - the QEP occurs at $\psi = y = 0$
- $F(\psi)$ is called the scaling function
- $f(\psi) \equiv k_F \times F(\psi)$ super-scaling function. In the RFG model $f(\psi) = \frac{3}{4}(1-\psi^2)$.

Definitions

- Inclusive electromagnetic reduced cross section $F(q,\omega) \equiv \frac{d^2\sigma/d\omega d\Omega}{\sigma_M(v_L G_L + v_T G_T)}$
  $d^2\sigma/d\omega d\Omega = \sigma_{Mott}\,(v_L R_L + v_T R_T)$
  $R_{L,T}(q,\omega)$ Longitudinal and Transverse nuclear response functions
  $G_{L,T}(q,\omega)$ elementary functions depending on the nucleonic form factors
  $v_{L,T}(q,\omega,\theta)$ kinematical factors
- If F becomes function of only one variable, scaling of first kind occurs
- This variable, a combination of q and ω, is called scaling variable
  - $y(q,\omega) \rightarrow$ minimum missing momentum
  - $\psi(q,\omega;k_F) \rightarrow$ minimum kinetic energy of the initial nucleon divided by the Fermi kinetic energy (dimensionless)
  - $\psi \simeq y/k_F$
  - the QEP occurs at $\psi = y = 0$
- $F(\psi)$ is called the scaling function
- $f(\psi) \equiv k_F \times F(\psi)$ super-scaling function. In the RFG model $f(\psi) = \frac{3}{4}(1-\psi^2)$.
- If f is independent of k_F, scaling of second kind occurs $\implies$ $\sigma \sim A/k_F$

Definitions

- Inclusive electromagnetic reduced cross section $F(q,\omega) \equiv \frac{d^2\sigma/d\omega d\Omega}{\sigma_M(v_L G_L + v_T G_T)}$
  $d^2\sigma/d\omega d\Omega = \sigma_{Mott}\,(v_L R_L + v_T R_T)$
  $R_{L,T}(q,\omega)$ Longitudinal and Transverse nuclear response functions
  $G_{L,T}(q,\omega)$ elementary functions depending on the nucleonic form factors
  $v_{L,T}(q,\omega,\theta)$ kinematical factors
- If F becomes function of only one variable, scaling of first kind occurs
- This variable, a combination of q and ω, is called scaling variable
  - $y(q,\omega) \rightarrow$ minimum missing momentum
  - $\psi(q,\omega;k_F) \rightarrow$ minimum kinetic energy of the initial nucleon divided by the Fermi kinetic energy (dimensionless)
  - $\psi \simeq y/k_F$
  - the QEP occurs at $\psi = y = 0$
- $F(\psi)$ is called the scaling function
- $f(\psi) \equiv k_F \times F(\psi)$ super-scaling function. In the RFG model $f(\psi) = \frac{3}{4}(1-\psi^2)$.
- If f is independent of k_F, scaling of second kind occurs $\implies$ $\sigma \sim A/k_F$
- Scaling of I and II kind $\implies$ Superscaling

Scaling of first kind (independence of q)

Day *et al.*, Annu. Rev. Nucl. Part. Sci. (1990)

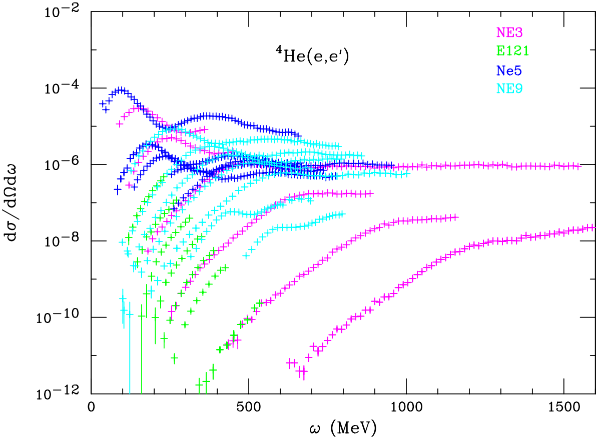

$$\omega_{QEP} = \frac{Q^2}{2m_N}$$

Scaling of first kind (independence of q)

Day *et al.*, Annu. Rev. Nucl. Part. Sci. (1990)

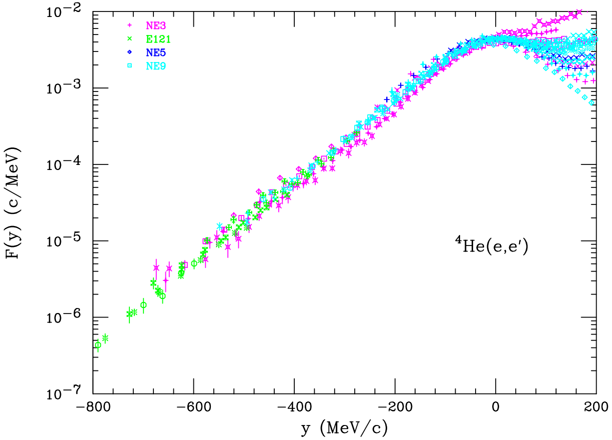

$y_{QEP} = 0$
Scaling is good at energy loss below the QEP ($y < 0$) and broken at $y > 0$.

Scaling of first kind (independence of q)

Day *et al.*, Annu. Rev. Nucl. Part. Sci. (1990)

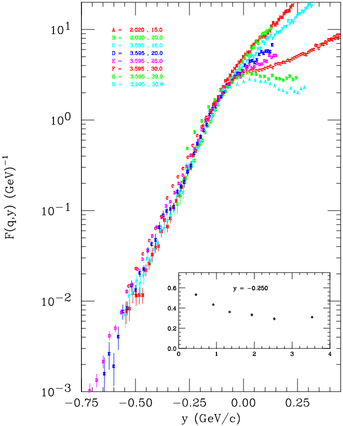

Data on Fe. The insert shows the convergence of $F(q, y)$ as a function of $Q^2[GeV^2/c^2]$.

Scaling of second kind (independence of A)

Donnelly and Sick, PRL82 & PRC60 (1999)

$f = k_F \times F$

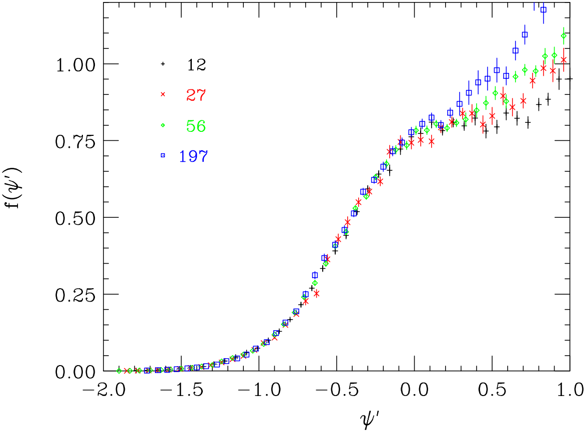

Data at E_e=3.6 GeV, θ=36 deg ($q \sim$1 GeV/c); $\psi' \equiv \psi(\omega \to \omega - E_{shift})$

Scaling of first and second kind

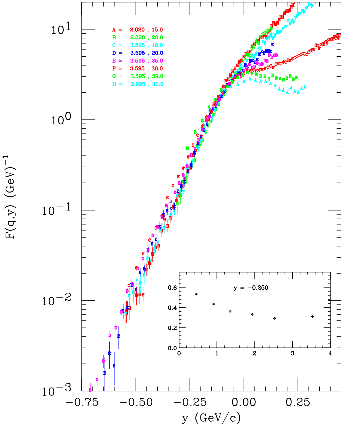

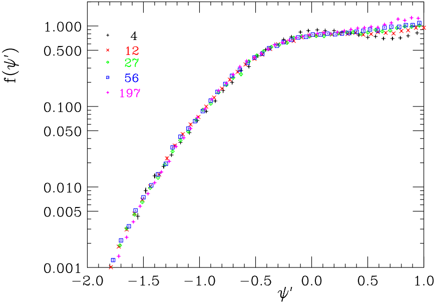

Scaling of second kind is realized better than first kind, with violations at $\psi' > 0$.

Scaling of zero-th kind? L/T separation

Day *et al.*, Annu. Rev. Nucl. Part. Sci. (1990) $F_{L,T} = R_{L,T}/G_{L,T}$

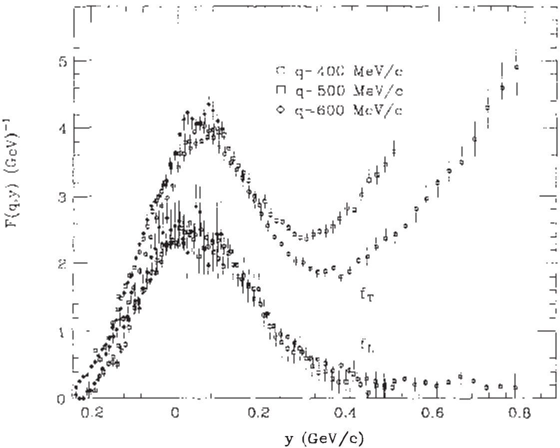

Figure 12 $F_{L,T}(q,y)$ for C at three different momentum transfers (57). The longitudinal and transverse scaling functions scale separately; the transverse is enhanced relative to the longitudinal in apparent violation of the PWIA. Data from Ref. 90.

Superscaling in the Longitudinal and Transverse channels

Donnelly and Sick, PRL82 & PRC60 (1999)

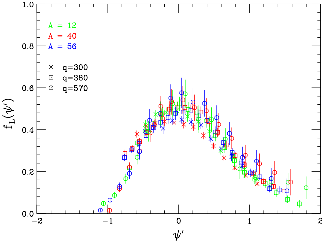

Superscaling in the Longitudinal and Transverse channels

Donnelly and Sick, PRL82 & PRC60 (1999)

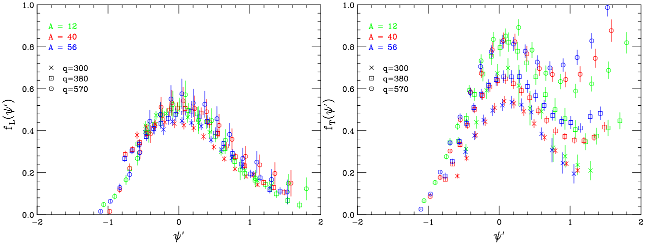

Superscaling in the Longitudinal and Transverse channels

Donnelly and Sick, PRL82 & PRC60 (1999)

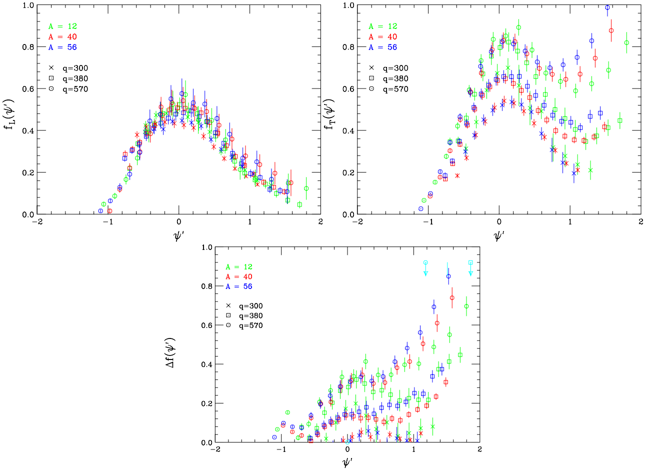

- $f_T > f_L$
- Violations reside mainly in the transverse channel (2p2h MEC, Δ resonance excitation, ...)

Contents

2p-2h MEC model

- The 2p2h response corresponds to the absorption of the vector boson from the leptonic current by a pair of nucleons (2-body current)

2p-2h MEC model

- The 2p2h response corresponds to the absorption of the vector boson from the leptonic current by a pair of nucleons (2-body current)
- Our 2p2h model is based on the calculation A. De Pace et al., (2003) performed for electron scattering and recently extended to the weak sector [I. Ruiz Simo et al., (2016)]

2p-2h MEC model

- The 2p2h response corresponds to the absorption of the vector boson from the leptonic current by a pair of nucleons (2-body current)
- Our 2p2h model is based on the calculation A. De Pace et al., (2003) performed for electron scattering and recently extended to the weak sector [I. Ruiz Simo et al., (2016)]
- The MEC considered are those carried by the pion and Δ degrees of freedom

2p-2h MEC model

- The 2p2h response corresponds to the absorption of the vector boson from the leptonic current by a pair of nucleons (2-body current)
- Our 2p2h model is based on the calculation A. De Pace et al., (2003) performed for electron scattering and recently extended to the weak sector [I. Ruiz Simo et al., (2016)]
- The MEC considered are those carried by the pion and Δ degrees of freedom
- All 2p-2h many-body diagrams containing two pionic lines are included

2p-2h MEC model

- The 2p2h response corresponds to the absorption of the vector boson from the leptonic current by a pair of nucleons (2-body current)
- Our 2p2h model is based on the calculation A. De Pace et al., (2003) performed for electron scattering and recently extended to the weak sector [I. Ruiz Simo et al., (2016)]
- The MEC considered are those carried by the pion and Δ degrees of freedom
- All 2p-2h many-body diagrams containing two pionic lines are included
- The calculation is performed in the RFG model in which Lorentz covariance can be maintained

2p-2h MEC model

- The 2p2h response corresponds to the absorption of the vector boson from the leptonic current by a pair of nucleons (2-body current)
- Our 2p2h model is based on the calculation A. De Pace et al., (2003) performed for electron scattering and recently extended to the weak sector [I. Ruiz Simo et al., (2016)]
- The MEC considered are those carried by the pion and Δ degrees of freedom
- All 2p-2h many-body diagrams containing two pionic lines are included
- The calculation is performed in the RFG model in which Lorentz covariance can be maintained
- Although based on the simple RFG, it is computationally non-trivial and involves 7D integrals of many terms. Comparison with neutrino scattering data implies one additional integral over the neutrino flux

2p-2h MEC model

- The 2p2h response corresponds to the absorption of the vector boson from the leptonic current by a pair of nucleons (2-body current)
- Our 2p2h model is based on the calculation A. De Pace et al., (2003) performed for electron scattering and recently extended to the weak sector [I. Ruiz Simo et al., (2016)]
- The MEC considered are those carried by the pion and Δ degrees of freedom
- All 2p-2h many-body diagrams containing two pionic lines are included
- The calculation is performed in the RFG model in which Lorentz covariance can be maintained
- Although based on the simple RFG, it is computationally non-trivial and involves 7D integrals of many terms. Comparison with neutrino scattering data implies one additional integral over the neutrino flux
- De Pace et al. technique: polarization propagator, many-body Goldstone diagrams, analytic manipulation of isospin traces and Dirac matrices spin traces using FORM, Monte Carlo integration
- Amaro et al. technique: numerical evaluation of the hadronic tensor $W^{\mu\nu}_{2p2h}$, including the spin traces. The contributions of pp, nn, pn channels can be separated.

Two-body meson exchange currents: elementary diagrams

"Seagull" and
"Pion-in-flight"

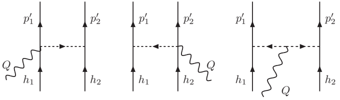

(a) (b) (c)

"Pion-pole"

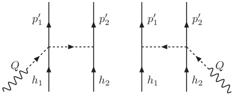

(d) (e)

"Δ-MEC"

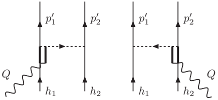

(f) (g)

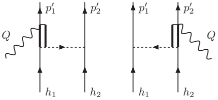

(h) (i)

De Pace et al. calculation

$$+F_{\pi NN}(\mathbf{k}_1^2)F_{\pi N\Delta}(\mathbf{k}_1^2)F_{\pi NN}(\mathbf{k}_2^2)F_{\pi N\Delta}(\mathbf{k}_2^2)A^2\frac{\mathbf{k}_{1T}^2\mathbf{q}^2}{(\mathbf{k}_1^2+\mu_\pi^2)(\mathbf{k}_2^2+\mu_\pi^2)}\Bigg]$$

$$+(1\leftrightarrow 2)\Bigg\}, \tag{18}$$

where the first two terms on the right-hand side correspond to the diagrams (a)–(c) of Fig. 4, and the last one to the diagrams (d)–(f). In this case six distinct diagrams contribute.

In Eqs. (16), (17) and (18) $\mathbf{k}_L$ and $\mathbf{k}_T$ indicate the longitudinal and transverse components of the vector $\mathbf{k}$ with respect to the direction fixed by $\mathbf{q}$. Furthermore, in the appropriate places, the hadronic monopole form factors

$$F_{\pi NN}(k^2)=\frac{\Lambda_\pi^2-\mu_\pi^2}{\Lambda_\pi^2-k^2}, \tag{19a}$$

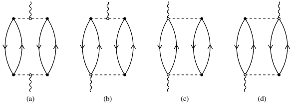

Fig. 2. The direct pionic contributions to the MEC 2p–2h response function.

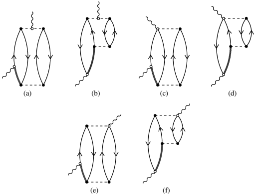

Fig. 3. The direct pionic/Δ interference contributions to the MEC 2p–2h response function.

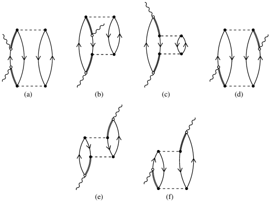

Fig. 4. The direct Δ contributions to the MEC 2p–2h response function.

$$F_{\pi N\Delta}(k^2)=\frac{\Lambda_{\pi N\Delta}^2}{\Lambda_{\pi N\Delta}^2-k^2} \tag{19b}$$

and the EM ones

$$F_{\gamma NN}(q^2)=\frac{1}{(1-q^2/\Lambda_D^2)^2}, \tag{19c}$$

$$F_{\gamma N\Delta}(q^2)=F_{\gamma NN}(q^2)\left(1-\frac{q^2}{\Lambda_2^2}\right)^{-1/2}\left(1-\frac{q^2}{\Lambda_3^2}\right)^{-1/2} \tag{19d}$$

have been introduced. In the non-relativistic expressions the hadronic form factors have been taken in the static limit. The cut-offs have been chosen as in DBT, namely $\Lambda_\pi=1300$ MeV, $\Lambda_{\pi N\Delta}=1150$ MeV, $\Lambda_D^2=0.71$ GeV^2, $\Lambda_2=M+M_\Delta$ and $\Lambda_3^2=3.5$ GeV^2. This choice clearly makes it possible a direct comparison between our results for R_T and those of DBT.

For completeness, we give also the formulae of the (smaller) exchange contributions to the integrand of Eq. (15), $\mathcal{R}_T^E(\mathbf{k}_1,\mathbf{k}_2;\mathbf{k}_1',\mathbf{k}_2';\mathbf{q},\omega)$, in the non-relativistic limit. The purely pionic contribution is identically zero, as a consequence of charge conservation and of the fact that the photon does not couple to a neutral pion. For the interference between pion and Δ (Fig. 5) we have

$$\mathcal{R}_T^{E(\pi\Delta)}(\mathbf{k}_1,\mathbf{k}_2;\mathbf{k}_1',\mathbf{k}_2';\mathbf{q},\omega)$$
$$=\frac{V^4}{(2M)^4}\sum_{\sigma\tau}\sum_{ij}\left(\delta_{ij}-\frac{q_iq_j}{\mathbf{q}^2}\right)\big[J_i^{\pi\dagger}(\mathbf{k}_1,\mathbf{k}_2)J_j^{\Delta}(\mathbf{k}_1',\mathbf{k}_2')$$
$$+J_i^{\Delta\dagger}(\mathbf{k}_1,\mathbf{k}_2)J_j^{\pi}(\mathbf{k}_1',\mathbf{k}_2')\big]$$

De Pace et al. calculation

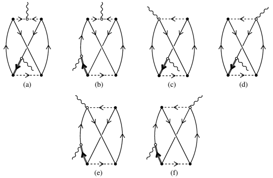

Fig. 5. The exchange pionic/Δ interference contributions to the MEC 2p–2h response function.

$$
\begin{aligned}
&= \frac{16 f_{\pi NN}^3 f_{\gamma\pi\pi} f_{\gamma N\Delta} f_{\pi N\Delta}}{3\mu_\pi^4 M} \\
&\quad \times B\boldsymbol{q}^2 \left\{ \frac{(\boldsymbol{k}_2 \times \boldsymbol{k}'_2)_L^2}{(\boldsymbol{k}_2^2+\mu_\pi^2)(\boldsymbol{k}'^2_2+\mu_\pi^2)} \left[\frac{1}{\boldsymbol{k}_1^2+\mu_\pi^2} + \frac{1}{\boldsymbol{k}'^2_1+\mu_\pi^2} \right] + (1 \leftrightarrow 2) \right\} \\
&\quad + \frac{8 f_{\pi NN}^3 f_{\gamma\pi NN} f_{\gamma N\Delta} f_{\pi N\Delta}}{3\mu_\pi^4 M} \\
&\quad \times B \left\{ \frac{(\boldsymbol{q}\cdot\boldsymbol{k}_2)\boldsymbol{k}'^2_2 + (\boldsymbol{q}\cdot\boldsymbol{k}'_2)\boldsymbol{k}_2^2 - (\boldsymbol{q}\cdot\boldsymbol{k}'_2)(\boldsymbol{k}_2\cdot\boldsymbol{k}'_2) - (\boldsymbol{q}\cdot\boldsymbol{k}_2)(\boldsymbol{k}_2\cdot\boldsymbol{k}'_2)}{(\boldsymbol{k}_2^2+\mu_\pi^2)(\boldsymbol{k}'^2_2+\mu_\pi^2)} \right. \\
&\quad + \frac{(\boldsymbol{q}\cdot\boldsymbol{k}_1)\boldsymbol{k}'^2_2 - (\boldsymbol{q}\cdot\boldsymbol{k}'_2)(\boldsymbol{k}_1\cdot\boldsymbol{k}'_2)}{(\boldsymbol{k}_1^2+\mu_\pi^2)(\boldsymbol{k}'^2_2+\mu_\pi^2)} + \frac{(\boldsymbol{q}\cdot\boldsymbol{k}'_1)\boldsymbol{k}_2^2 - (\boldsymbol{q}\cdot\boldsymbol{k}_2)(\boldsymbol{k}'_1\cdot\boldsymbol{k}_2)}{(\boldsymbol{k}'^2_1+\mu_\pi^2)(\boldsymbol{k}_2^2+\mu_\pi^2)} \\
&\quad \left. + (1 \leftrightarrow 2) \right\}.
\end{aligned}
\tag{20}
$$

The contribution of the Δ alone (Fig. 6) is instead

$$
\begin{aligned}
&\mathcal{R}_T^{E\Delta}(\boldsymbol{k}_1, \boldsymbol{k}_2; \boldsymbol{k}'_1, \boldsymbol{k}'_2; \boldsymbol{q}, \omega) \\
&\quad = \frac{V^4}{(2M)^4} \sum_{\sigma\tau} \sum_{ij} \left(\delta_{ij} - \frac{q_i q_j}{\boldsymbol{q}^2} \right) J_i^{\pi\dagger}(\boldsymbol{k}_1, \boldsymbol{k}_2) J_j^{\Delta}(\boldsymbol{k}'_1, \boldsymbol{k}'_2) \\
&\quad = \frac{4 f_{\pi NN}^2 f_{\pi N\Delta}^2 f_{\gamma N\Delta}^2}{9M^2\mu_\pi^4} \boldsymbol{q}^2 \left\{ B^2 \left[\frac{(\boldsymbol{k}_1\cdot\boldsymbol{k}'_1)(\boldsymbol{k}_{1T}\cdot\boldsymbol{k}'_{1T})}{(\boldsymbol{k}_1^2+\mu_\pi^2)(\boldsymbol{k}'^2_1+\mu_\pi^2)} + \frac{(\boldsymbol{k}_1\cdot\boldsymbol{k}'_2)(\boldsymbol{k}_{1T}\cdot\boldsymbol{k}'_{2T})}{(\boldsymbol{k}_1^2+\mu_\pi^2)(\boldsymbol{k}'^2_2+\mu_\pi^2)} \right. \right. \\
&\quad \left. + (1 \leftrightarrow 2) \right] + AB \left[\frac{2(\boldsymbol{k}_1 \times \boldsymbol{k}'_1)_L^2 - 2k_{1L}k'_{1L}(\boldsymbol{k}_1\cdot\boldsymbol{k}'_1) + k'^2_{1L}\boldsymbol{k}_1^2 + k_{1L}^2\boldsymbol{k}'^2_1}{(\boldsymbol{k}_1^2+\mu_\pi^2)(\boldsymbol{k}'^2_1+\mu_\pi^2)} \right.
\end{aligned}
$$

$$
\begin{aligned}
&\quad \times \frac{2(\boldsymbol{k}_1 \times \boldsymbol{k}'_2)_L^2 - 2k_{1L}k'_{2L}(\boldsymbol{k}_1\cdot\boldsymbol{k}'_2) + k'^2_{2L}\boldsymbol{k}_1^2 + k_{1L}^2\boldsymbol{k}'^2_2}{(\boldsymbol{k}_1^2+\mu_\pi^2)(\boldsymbol{k}'^2_2+\mu_\pi^2)} \\
&\quad \left. \left. + (1 \leftrightarrow 2) \right] \right\}.
\end{aligned}
\tag{21}
$$

Eqs. (16), (17) and (18) could in principle be compared with Eq. (5.11) of DBT; however, the overall normalization of the latter is not correct, since its dimension is not consistent with its definition (namely of being the transverse part of the amplitude $\mathcal{T}$ given in Eq. (4.8) of DBT); moreover, the relative weights of the interference and Δ contributions with respect to the pionic one differ, in our calculations, by a factor 2 and 4, respectively, from those of Eq. (5.11) of DBT. These factors, however, are not able to explain the marked difference between our results and those in that paper. Note that although the authors of DBT write down exactly the same expressions as we do for the non-relativistic MEC currents, actually they state that the non-relativistic procedure to get their Eq. (5.11) is applied at the level of the hadronic tensor, that is by reducing the (cumbersome) exact relativistic response.

In Fig. 7 we now compare our results with those of DBT, where the non-relativistic R_T (without the exchange contribution) is shown for $q = 550$ MeV$/c$ (left) and for $q = 1140$ MeV$/c$ (right), with an atomic mass number of 56 and utilizing a Fermi momentum $k_F = 1.3$ fm^{-1}. The latter value is employed for the sake of comparison with DBT, although in fact it is more appropriate for heavier nuclei.

It is clearly apparent in the figure that our predictions differ significantly from those of DBT: while the discrepancy is mild for moderate values of ω (roughly, those encompassing the QEP), it becomes striking at higher energies, namely in the region of the so-called dip and of the Δ-peak. Here our transverse response function in the proximity of the lightcone turns out to be larger by about a factor two at $q = 550$ MeV$/c$ and by over a factor three at $q = 1140$ MeV$/c$.

Note that, in order to conform as closely as possible with the DBT approach, we have accounted for the initial state binding of the two holes by phenomenologically inserting

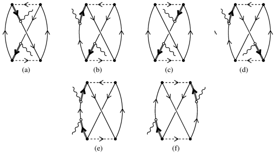

Fig. 6. The exchange Δ contributions to the MEC 2p–2h response function.

Amaro et al. calculation

Numerical evaluation of the 2p2h hadronic tensor

$$
\begin{aligned}
W^{\mu\nu}_{2p-2h} &= \frac{V}{(2\pi)^9}\int d^3p'_1 d^3h_1 d^3h_2 \frac{M^4}{E_1E_2E'_1E'_2} r^{\mu\nu}(\mathbf{p}'_1,\mathbf{p}'_2,\mathbf{h}_1,\mathbf{h}_2)\delta(E'_1+E'_2-E_1-E_2-\omega) \\
&\times \quad \theta(p'_2-k_F)\theta(p'_1-k_F)\theta(k_F-h_1)\theta(k_F-h_2)
\end{aligned}
$$

where $\mathbf{p'_2} = \mathbf{h_1} + \mathbf{h_2} + \mathbf{q} - \mathbf{p'_1}$ and the elementary hadronic tensor

$$
r^{\mu\nu}(\mathbf{p}'_1,\mathbf{p}'_2,\mathbf{h}_1,\mathbf{h}_2) = \frac{1}{4}\sum_{s_1s_2s'_1s'_2}\sum_{t_1t_2t'_1t'_2} j^\mu(1',2',1,2)^*_A j^\nu(1',2',1,2)_A.
$$

is given in terms of the antisymmetrized matrix element $j^\mu(1',2',1,2)_A$ of the 2-body current

$$
j^\mu_{\rm MEC} = j^\mu_{\rm sea} + j^\mu_\pi + j^\mu_{\rm pole} + j^\mu_\Delta
$$

involving Dirac spinors, γ matrices, pion and Δ propagators.

Comparison between Amaro and De Pace calculations

^{56}Fe

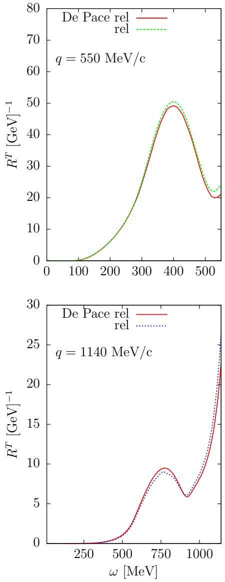

Scaling behavior of the 2p2h MEC response

De Pace *et al.*, Nucl.Phys. A741 (2004)

- The 2p2h MEC response breaks scaling of both kinds at $\psi > 0$

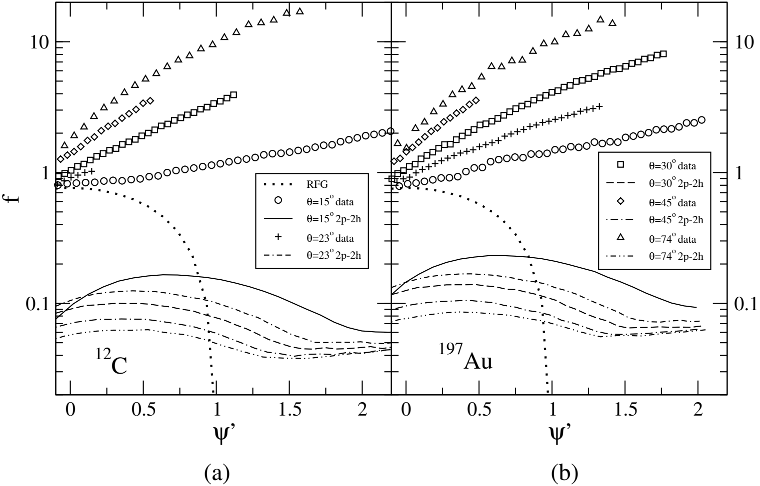

Scaling behavior of the 2p2h MEC response

De Pace *et al.*, Nucl.Phys. A741 (2004)

- ...and at large negative ψ

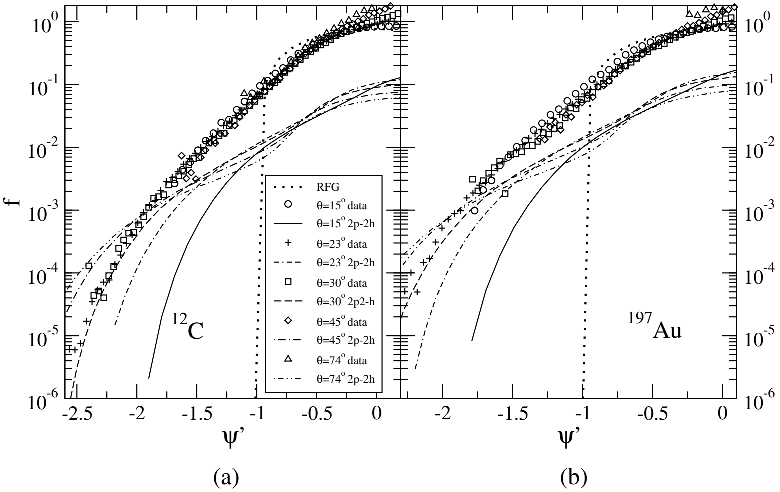

Scaling behavior of the 2p2h MEC response

Ann. of Phys. 131 (1981)

35 years ago

Carbon ⇒

Nickel ⇒

Lead ⇒

480 VAN ORDEN AND DONNELLY

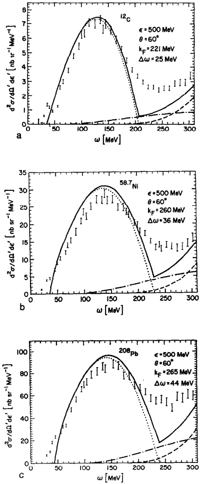

FIG. 10. Calculated cross sections for (a) ^{12}C, (b) $^{58.7}$Ni, and (c) ^{208}Pb, conditions as in Fig. 2, data from Ref. [8]. The dotted curve is the quasielastic contribution, the dash–dot curve the MEC contribution, the dashed curve the pion production contribution, and the solid curve the total.

Separated 2p2h $\Delta - \Delta$, $\pi - \pi$ and $\pi - \Delta$ contributions

k_F=200 MeV/c | k_F=300 MeV/c

q=0.8 GeV/c

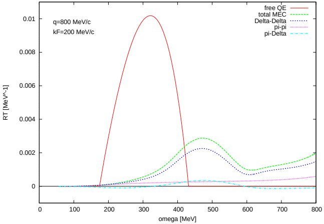

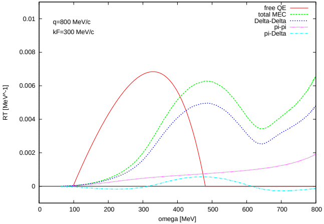

q=2.0 GeV/c

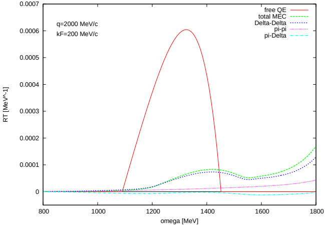

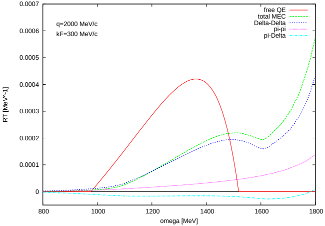

Scaling behavior of the 2p2h MEC response

The k_F dependence is more easily explored in the non-relativistic limit, where the 7D integrals reduce to 2D

Scaling behavior of the 2p2h MEC response

The k_F dependence is more easily explored in the non-relativistic limit, where the 7D integrals reduce to 2D

$$R^T_{2p-2h}(q,\omega) = \frac{V}{(2\pi)^6}\frac{k_F^7\, M}{q_F}\int_0^{x_{\max}}\frac{dx}{x^2}\int_{|q_F-x|}^{q_F+x}\frac{dy}{y^2}A(x,y,\nu)r^T(x,y),$$

where $\nu = m\omega/k_F^2$, $x_{\max} = 1+\sqrt{2(1+\nu)}$ and $q_F = \frac{q}{k_F}$ are dimensionless variables. The elementary 2p-2h response $r^T(x,y)$ is, in the e.m. case,

$$r^T = r^T_{\rm sea} + r^T_\pi + r^T_\Delta + r^T_{{\rm sea},\pi} + r^T_{{\rm sea},\Delta} + r^T_{\pi,\Delta}$$

and depends non-trivially upon k_F. For instance the seagull term is

$$r^T_{\rm sea}(x,y) = \left(2\frac{f^2_{\pi NN}}{m^2_\pi}F^V_1\right)^2\frac{8}{k_F^2}\left[\frac{x^2}{(x^2+m_F^2)^2}+\frac{y^2}{(y^2+m_F^2)^2}+\frac{x_T^2}{(x^2+m_F^2)(y^2+m_F^2)}\right],$$

where $m_F \equiv m_\pi/k_F$ and $x_T^2 = x^2 - \left(q_F^2+x^2-y^2\right)^2/(2q_F)^2$.

Scaling behavior of the 2p2h MEC response

The k_F dependence is more easily explored in the non-relativistic limit, where the 7D integrals reduce to 2D

$$R^T_{2p-2h}(q,\omega) = \frac{V}{(2\pi)^6}\frac{k_F^7 M}{q_F}\int_0^{x_{\max}}\frac{dx}{x^2}\int_{|q_F-x|}^{q_F+x}\frac{dy}{y^2}A(x,y,\nu)r^T(x,y),$$

where $\nu = m\omega/k_F^2$, $x_{\max} = 1+\sqrt{2(1+\nu)}$ and $q_F = \frac{q}{k_F}$ are dimensionless variables. The elementary 2p-2h response $r^T(x,y)$ is, in the e.m. case,

$$r^T = r^T_{\rm sea} + r^T_\pi + r^T_\Delta + r^T_{{\rm sea},\pi} + r^T_{{\rm sea},\Delta} + r^T_{\pi,\Delta}$$

and depends non-trivially upon k_F. For instance the seagull term is

$$r^T_{\rm sea}(x,y) = \left(2\frac{f^2_{\pi NN}}{m^2_\pi}F^V_1\right)^2\frac{8}{k_F^2}\left[\frac{x^2}{(x^2+m_F^2)^2}+\frac{y^2}{(y^2+m_F^2)^2}+\frac{x_T^2}{(x^2+m_F^2)(y^2+m_F^2)}\right],$$

where $m_F \equiv m_\pi/k_F$ and $x_T^2 = x^2 - \left(q_F^2+x^2-y^2\right)^2/(2q_F)^2$.

Three scales: m_N, m_π, q $\Longrightarrow$ Numerical studies are necessary.

Scaling behavior of the 2p2h MEC response

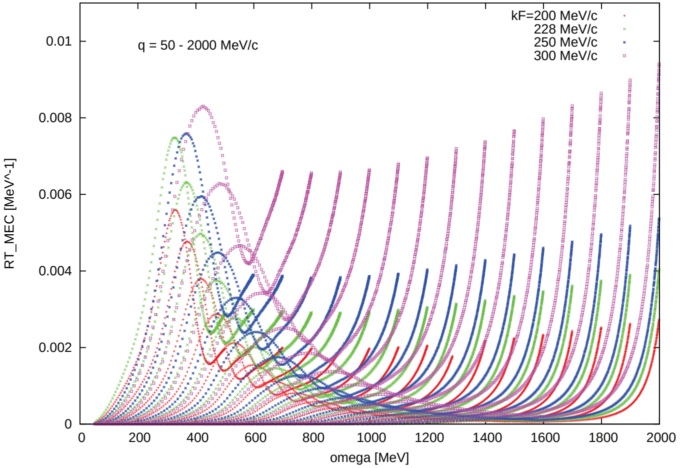

Scaling behavior of the 2p2h MEC response

Define $f_T^{MEC} \equiv (k_F/m_N)^\alpha \times R_T^{MEC}/\tilde{G}_M^2$ and vary α to find a scaling law.

Scaling behavior of the 2p2h MEC response

Define $f_T^{MEC} \equiv (k_F/m_N)^\alpha \times R_T^{MEC}/\tilde{G}_M^2$ and vary α to find a scaling law.
$\alpha = -2 \longrightarrow R_T^{MEC} \sim k_F^2$

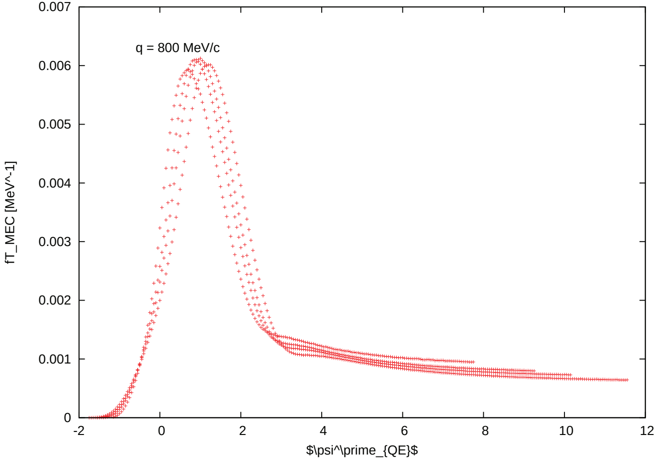

Scaling behavior of the 2p2h MEC response

The 2p2h response scales even better if plotted as a function of a variable $\psi'_{\rm MEC}$ devised for this kinematical region.

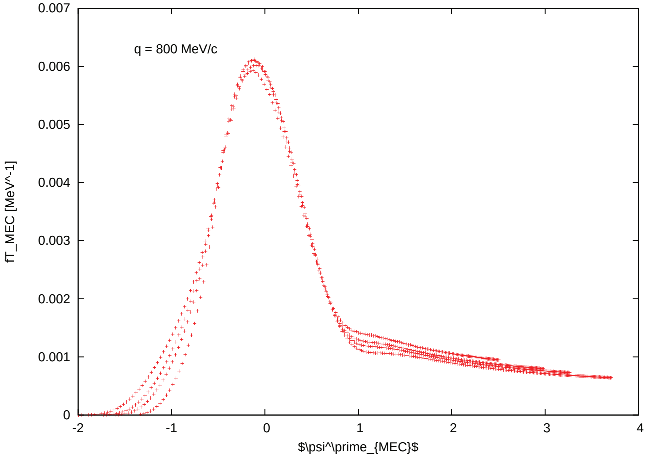

ψ-scaling variables

- **QE:**

$$\psi'_{\rm QE}(q,\omega;k_F) \equiv \frac{1}{\sqrt{\xi_F}} \frac{\lambda' - \tau'}{\sqrt{(1+\lambda')\tau' + \kappa\sqrt{\tau'(1+\tau')}}},$$

$\lambda' \equiv \frac{\omega'}{2m_N}$, $\kappa \equiv \frac{q}{2m_N}$, $\tau' \equiv \kappa^2 - \lambda'^2$, $\omega' \equiv \omega - E^{shift}$, $\xi_F \equiv \frac{E_F}{m_N} - 1$
E^{shift} is a parameter such that the maxima of QEP at different q align at $\psi' = 0$.

ψ-scaling variables

- **QE:**

$$\psi'_{\rm QE}(q,\omega;k_F) \equiv \frac{1}{\sqrt{\xi_F}} \frac{\lambda'-\tau'}{\sqrt{(1+\lambda')\tau'+\kappa\sqrt{\tau'(1+\tau')}}},$$

$\lambda' \equiv \frac{\omega'}{2m_N}$, $\kappa \equiv \frac{q}{2m_N}$, $\tau' \equiv \kappa^2 - \lambda'^2$, $\omega' \equiv \omega - E^{shift}$, $\xi_F \equiv \frac{E_F}{m_N} - 1$

E^{shift} is a parameter such that the maxima of QEP at different q align at $\psi' = 0$.

- **2p2h-MEC:**

$$\psi'_{\rm MEC}(q,\omega,k_F) \equiv \frac{1}{\sqrt{\xi_F^{eff}}} \frac{\lambda'_{\rm MEC} - \tau'_{\rm MEC}\rho'_{\rm MEC}}{\sqrt{(1+\lambda'_{\rm MEC}\rho'_{\rm MEC})\tau'_{\rm MEC} + \kappa\sqrt{\tau'_{\rm MEC}\left(1+\tau'_{\rm MEC}\rho'^{\,2}_{\rm MEC}\right)}}},$$

$\lambda'_{\rm MEC} \equiv \frac{\omega'_{\rm MEC}}{2m_N}$, $\kappa \equiv \frac{q}{2m_N}$, $\tau'_{\rm MEC} \equiv \kappa^2 - (\lambda'_{\rm MEC})^2$,

$\omega'_{\rm MEC} \equiv \omega - E^{shift}_{\rm MEC}$, $\rho'_{\rm MEC} \equiv 1 + \frac{1}{4\tau'_{\rm MEC}}\left(\frac{m_*^2}{m_N^2} - 1\right)$

The parameters m_*, ξ_F^{eff} and $E^{shift}_{\rm MEC}$ are chosen in such a way that the maxima of the 2p2h response at different values of q align at $\psi'_{\rm MEC} = 0$.

k_F dependence of the 2p-2h MEC responses

$\eta_F = k_F/m_N$: $R^T_{MEC}(\psi'_{MEC}) \sim \eta_F^2$ at the peak, with some violations in the tails

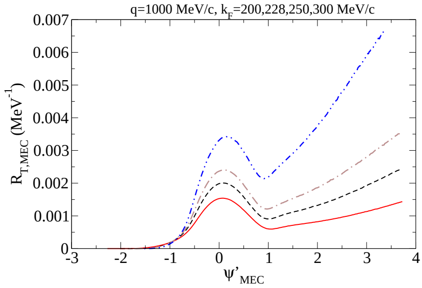

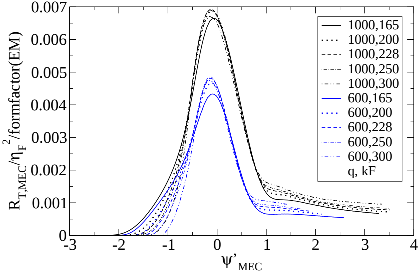

A parametrization of this behavior in terms of k_F (work in progress) could be valuable to extend our calculation to other nuclei without further theoretical calculations reducing significantly the computational time.

Scaling behavior of the 2p2h MEC response

Van Orden and Donnelly, Ann. of Phys. 131 (1981)

By expressing the quasielastic, MEC, and pion production contributions in terms of dimensionless variables (as done for the MEC in Section 2), it is found that the one-body QE and pion production contributions scale roughly as A/k_F^2, while the MEC scales as Ak_F^2. Careful comparison of Figs. 10a–c shows that the size of the MEC contribution relative to the QE peak increases considerably going from ^{12}C, where $k_F = 221$ MeV, to $^{58.7}$Ni, where $k_F = 260$ MeV, but that there is very little increase in relative size when going from $^{58.7}$Ni to ^{208}Pb, where $k_F = 265$ MeV. Thus, for lighter nuclei, where k_F is changing more rapidly with increasing A, the size of the MEC relative to the QE peak changes noticeably as A becomes larger. As A increases toward heavier nuclei, the nuclear density saturates, causing k_F to slowly approach the nuclear matter value of $k_F = 270$ MeV. This implies that for heavier nuclei all contributions will scale approximately as A. Therefore, while the relative MEC contribution will be largest for heavy nuclei, it changes most rapidly when comparing cross sections for light nuclei.

Scaling behavior of the 2p2h MEC response

Van Orden and Donnelly, Ann. of Phys. 131 (1981)

By expressing the quasielastic, MEC, and pion production contributions in terms of dimensionless variables (as done for the MEC in Section 2), it is found that the one-body QE and pion production contributions scale roughly as A/k_F^2, while the MEC scales as Ak_F^2. Careful comparison of Figs. 10a–c shows that the size of the MEC contribution relative to the QE peak increases considerably going from ^{12}C, where $k_F = 221$ MeV, to $^{58.7}$Ni, where $k_F = 260$ MeV, but that there is very little increase in relative size when going from $^{58.7}$Ni to ^{208}Pb, where $k_F = 265$ MeV. Thus, for lighter nuclei, where k_F is changing more rapidly with increasing A, the size of the MEC relative to the QE peak changes noticeably as A becomes larger. As A increases toward heavier nuclei, the nuclear density saturates, causing k_F to slowly approach the nuclear matter value of $k_F = 270$ MeV. This implies that for heavier nuclei all contributions will scale approximately as A. Therefore, while the relative MEC contribution will be largest for heavy nuclei, it changes most rapidly when comparing cross sections for light nuclei.

Maieron, Donnelly, Sick, PRC65 (2002)

TABLE I. Adjusted parameters.

Nucleus	k_F (MeV/c)	E_{shift} (MeV)
Lithium	165	15
Carbon	228	20
Magnesium	230	25
Aluminum	236	18
Calcium	241	28
Iron	241	23
Nickel	245	30
Tin	245	28
Gold	245	25
Lead	248	31

$k_F(A)$

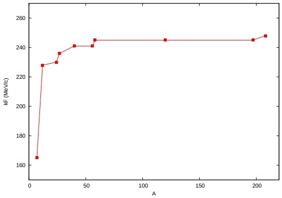

Separated charge channels in the 2p2h response

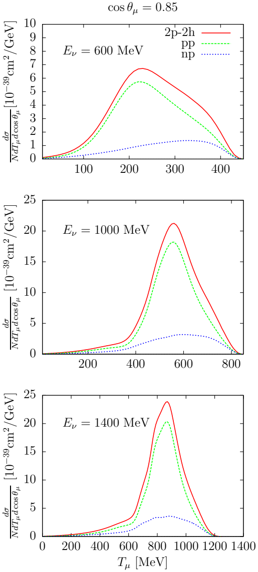

- pp final state largely dominate over np
- The ratio depends upon the kinematics
- The np cross section is shifted towards higher values of T_μ
- First step towards the treatment of $Z \neq N$ nuclei

Ruiz Simo et al., PLB762 (2016)

The SuSAv2 + MEC model

The Superscaling model

- The SuSA model is based on the quasielastic longitudinal superscaling function extracted from averaged separated world data on ^{12}C, ^{40}Ca, ^{56}Fe
- It contains corrections based on the Relativistic Mean Field model (SuSAv2)

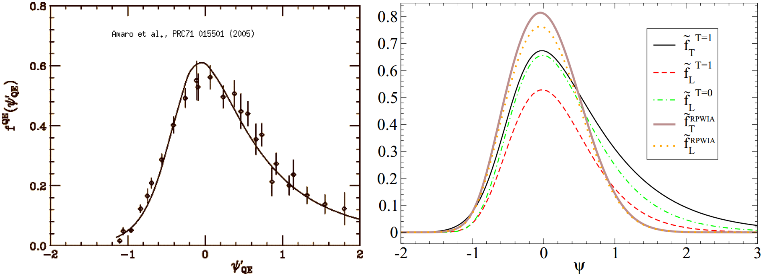

SuSA (left) and SuSAv2 (right) scaling functions

- 2p2h excitation induced by two-body currents (MEC), not included in the above models, are added as previously described

The inelastic region

The Superscaling approach can be extended to the inelastic spectrum in two ways:

The inelastic region

The Superscaling approach can be extended to the inelastic spectrum in two ways:

- employing phenomenological fits of the single-nucleon inelastic structure functions and assuming that the scaling function is the same in all energy regions $\longrightarrow$ full spectrum (from the Δ resonance to DIS)
  [MBB et al., PRC69, 035502, 2004; Megias et al., PRD94 013012, 2016]

The inelastic region

The Superscaling approach can be extended to the inelastic spectrum in two ways:

- employing phenomenological fits of the single-nucleon inelastic structure functions and assuming that the scaling function is the same in all energy regions ⟶ full spectrum (from the Δ resonance to DIS)
  [MBB et al., PRC69, 035502, 2004; Megias et al., PRD94 013012, 2016]
- constructing a phenomenological scaling function to be used in the Δ-resonance region
  [Ivanov et al., Phys.Lett. B711 (2012)]

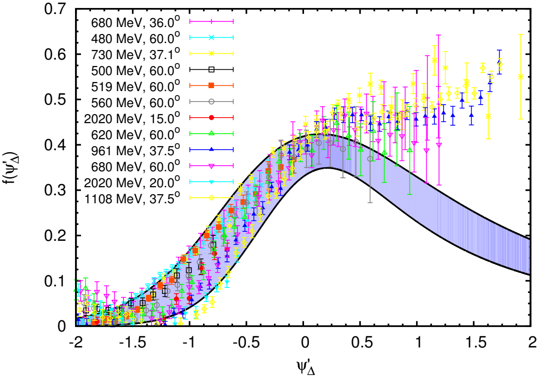

Formalism: response functions

- Double differential CC ν $(+)$ and $\overline{\nu}$ (-) cross section

$$\left[\frac{d\sigma}{dk_\mu d\Omega}\right]_\pm = \sigma_0 \mathcal{F}_\pm^2 \quad ; \quad \sigma_0 = \frac{\left(G_F^2 \cos\theta_c\right)^2}{2\pi^2}\left(k_\mu \cos\frac{\tilde{\theta}}{2}\right)^2$$

Formalism: response functions

- Double differential CC ν (+) and $\overline{\nu}$ (-) cross section

$$\left[\frac{d\sigma}{dk_\mu d\Omega}\right]_\pm = \sigma_0 \mathcal{F}_\pm^2 \quad ; \quad \sigma_0 = \frac{\left(G_F^2 \cos\theta_c\right)^2}{2\pi^2}\left(k_\mu \cos\frac{\tilde{\theta}}{2}\right)^2$$

- Rosenbluth-like decomposition: 3 responses

$$\mathcal{F}_\pm^2 = \hat{V}_L R_L + \hat{V}_T R_T \pm \left[2\hat{V}_{T'} R_{T'}\right]$$

$$\hat{V}_L R_L = V_{CC} R_{CC} + V_{CL} R_{CL} + V_{LL} R_{LL}$$

with

$R_L = R_L^{VV} + R_L^{AA}$ VV (vector-vector)

$R_T = R_T^{VV} + R_T^{AA}$ AA (axial-axial)

$R_{T'} = R_{T'}^{VA}$ VA (vector-axial)

from the V and A weak leptonic and hadronic currents $j^\mu = j_V^\mu + j_A^\mu$; $J^\mu = J_V^\mu + J_A^\mu$

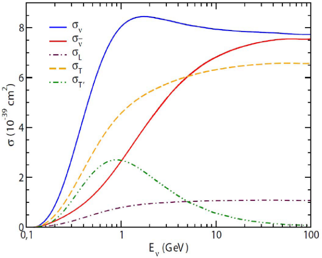

Validation with electron scattering data (G. Megias' talk)

Megias *et al.*, PRD 94, 013012 (2016)

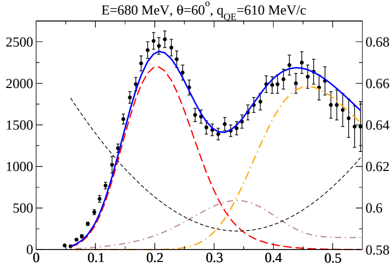

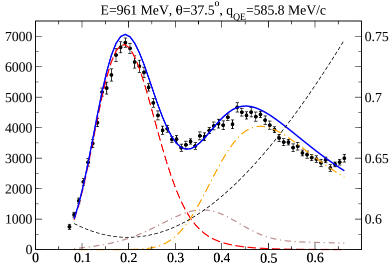

e-C data from Day *et al.*, http://faculty.virginia.edu/qes-archive/

Contents

MiniBooNE CCQE

MiniBooNE ν_μ-C

Megias *et al.*, PRD 94, 093004 (2016)

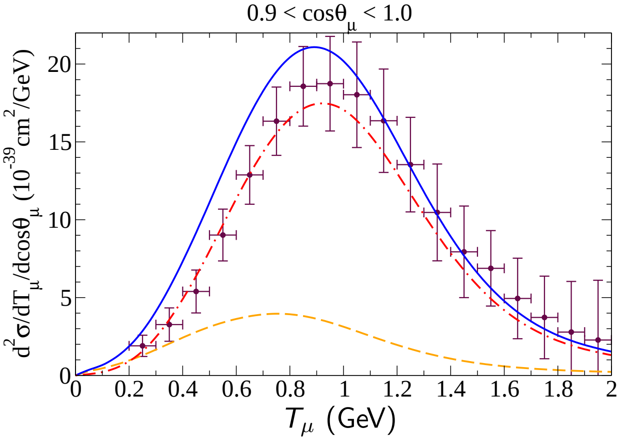

MiniBooNE $\bar{\nu}_\mu$-C

Megias *et al.*, PRD 94, 093004 (2016)

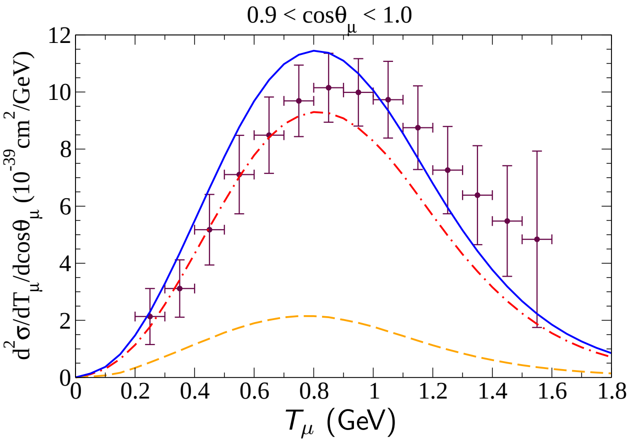

$\nu_\mu - C$

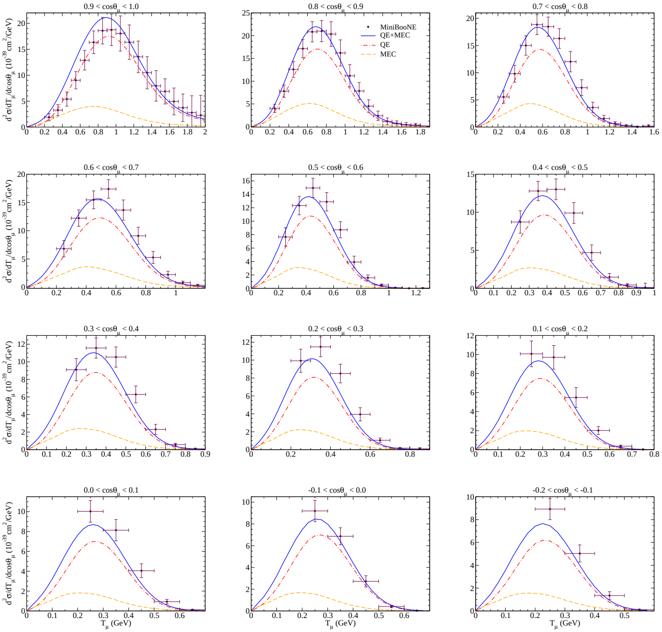
0.9 < cosθ_μ < 1.0
0.8 < cosθ_μ < 0.9
0.7 < cosθ_μ < 0.8
0.6 < cosθ_μ < 0.7
0.5 < cosθ_μ < 0.6
0.4 < cosθ_μ < 0.5
0.3 < cosθ_μ < 0.4
0.2 < cosθ_μ < 0.3
0.1 < cosθ_μ < 0.2
0.0 < cosθ_μ < 0.1
-0.1 < cosθ_μ < 0.0
-0.2 < cosθ_μ < -0.1
MiniBooNE
QE+MEC
QE
MEC
d²σ/dT_μ/dcosθ_μ (10⁻³⁹ cm²/GeV)
T_μ (GeV)

$\bar{\nu}_\mu - C$

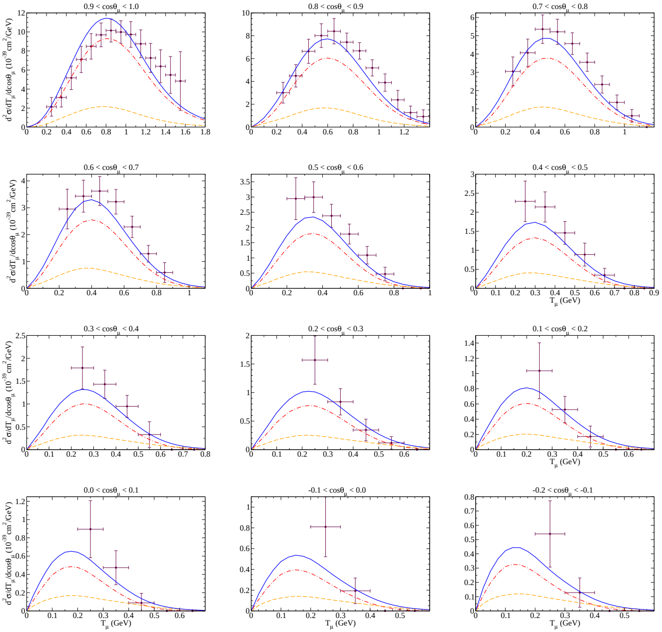
0.9 < cosθ_μ < 1.0
0.8 < cosθ_μ < 0.9
0.7 < cosθ_μ < 0.8
0.6 < cosθ_μ < 0.7
0.5 < cosθ_μ < 0.6
0.4 < cosθ_μ < 0.5
0.3 < cosθ_μ < 0.4
0.2 < cosθ_μ < 0.3
0.1 < cosθ_μ < 0.2
0.0 < cosθ_μ < 0.1
-0.1 < cosθ_μ < 0.0
-0.2 < cosθ_μ < -0.1
d²σ/dT_μ/dcosθ_μ (10⁻³⁹ cm²/GeV)
T_μ (GeV)

MiniBooNE ν_μ-C

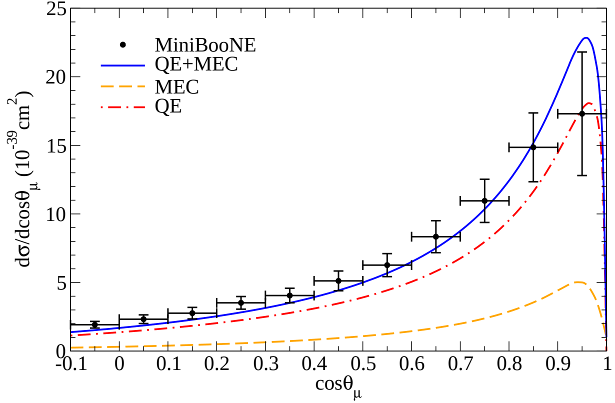

MiniBooNE ν_μ-C

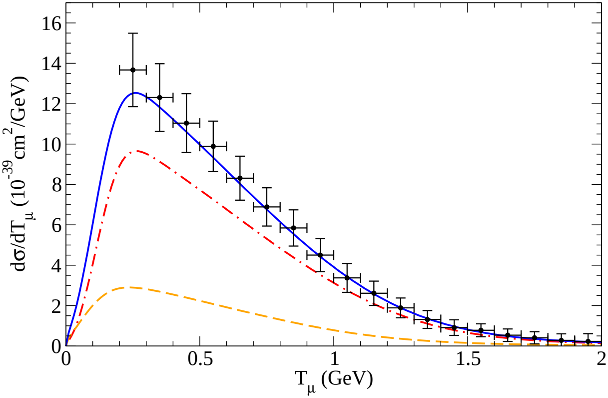

MiniBooNE $\bar{\nu}_\mu$-C

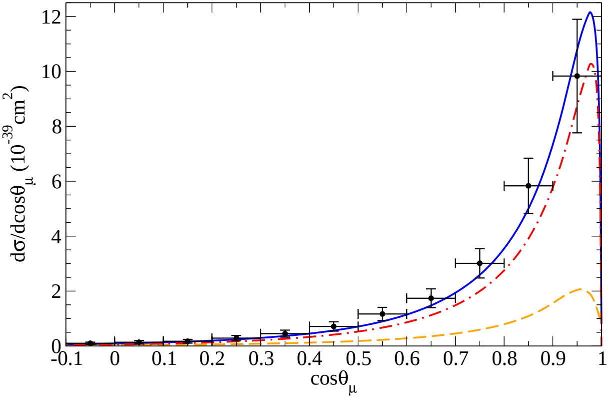

MiniBooNE $\bar{\nu}_\mu$-C

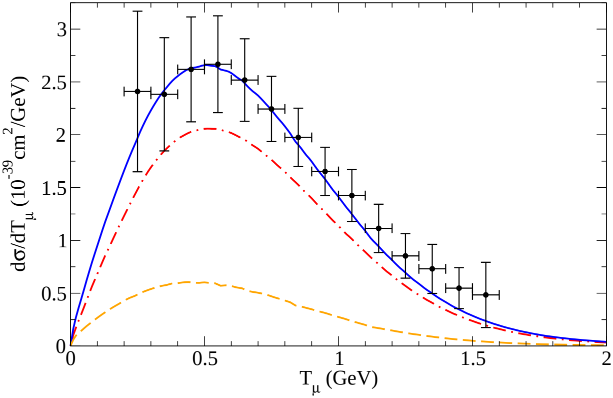

MINERνA CCQE

MINERνA

Megias *et al.*, PRD 94, 093004 (2016)

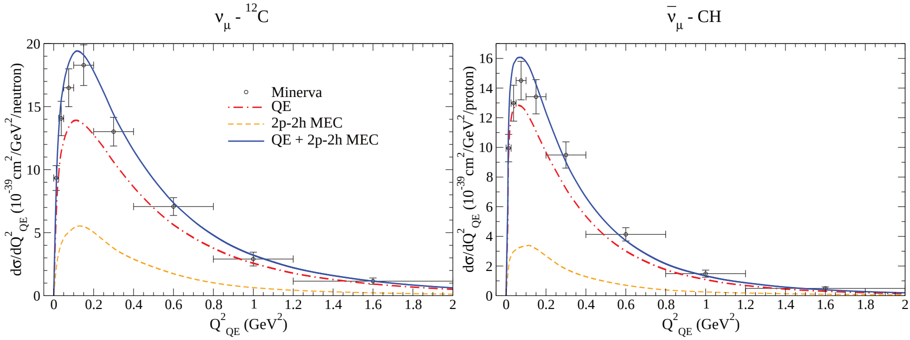

MinerνA ν_e-C

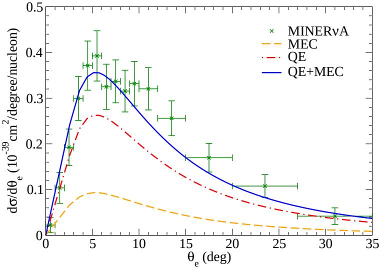

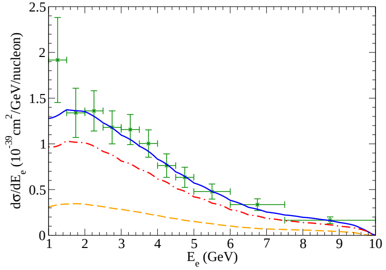

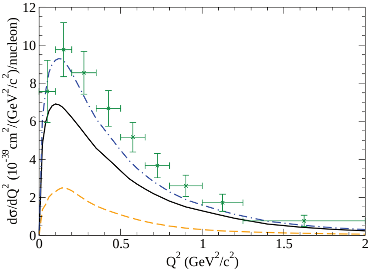

T2K CCQE

T2K ν_μ-C

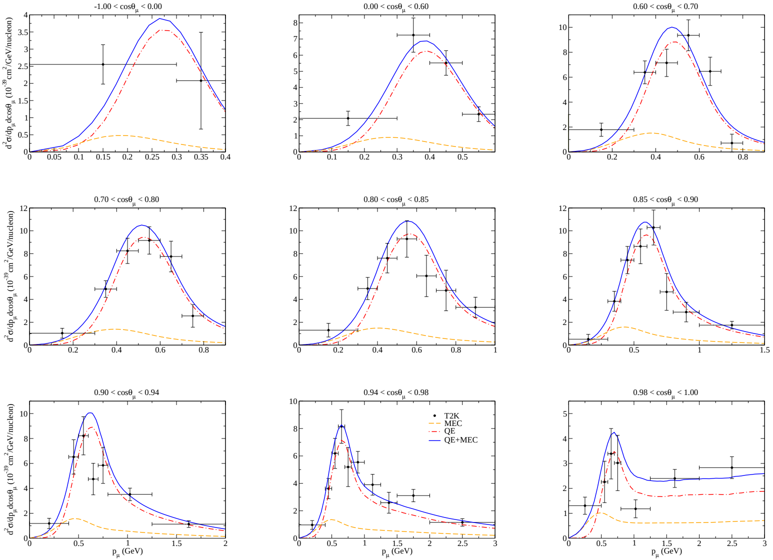
-1.00 < cosθμ < 0.00
0.00 < cosθμ < 0.60
0.60 < cosθμ < 0.70
0.70 < cosθμ < 0.80
0.80 < cosθμ < 0.85
0.85 < cosθμ < 0.90
0.90 < cosθμ < 0.94
0.94 < cosθμ < 0.98
0.98 < cosθμ < 1.00
d²σ/dpμdcosθμ (10⁻³⁹cm²/GeV/nucleon)
pμ (GeV)
T2K
MEC
QE
QE+MEC

T2K CC-inclusive

T2K inclusive ν_μ-C

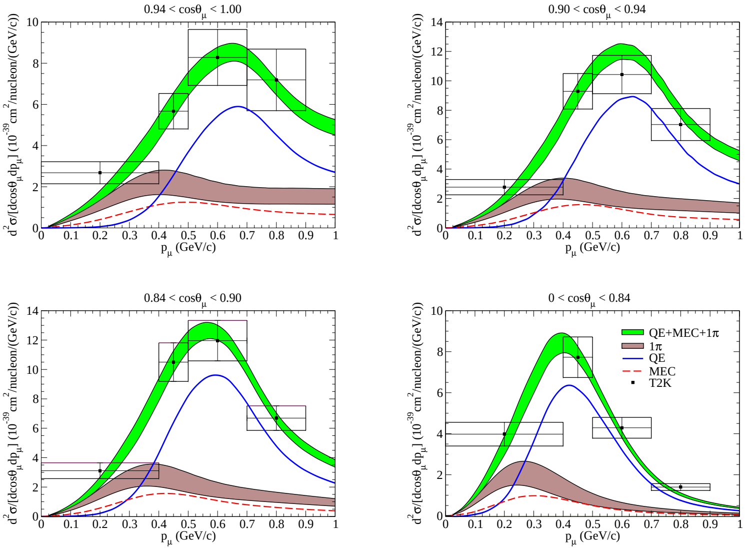

T2K ν_e-C

Megias *et al.*, PRD 94, 093004 (2016)

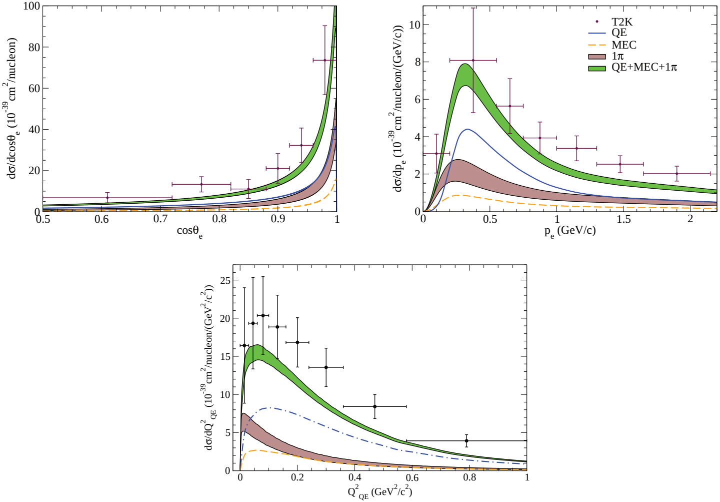

Summary

- Superscaling is a valuable tool to connect electron and neutrino scattering
- MEC 2p2h contributions violates scaling of both kinds
- Numerical studies suggest that the ratio 2body/1body roughly scales as k_F^3
- Comparison of the SuSAv2+MEC model with inclusive electron scattering data on ^{12}C is very satisfactory in a wide range of kinematics
- Fair agreement of the SuSAv2+MEC predictions with CCQE-like neutrino scattering data on ^{12}C
- Work in progress: extension to asymmetric nuclei, inclusive neutrino scattering including all inelasticities

Summary

- Superscaling is a valuable tool to connect electron and neutrino scattering
- MEC 2p2h contributions violates scaling of both kinds
- Numerical studies suggest that the ratio 2body/1body roughly scales as k_F^3
- Comparison of the SuSAv2+MEC model with inclusive electron scattering data on ^{12}C is very satisfactory in a wide range of kinematics
- Fair agreement of the SuSAv2+MEC predictions with CCQE-like neutrino scattering data on ^{12}C
- Work in progress: extension to asymmetric nuclei, inclusive neutrino scattering including all inelasticities

Thank you

Backup slides

Comparison with ^{12}C (e,e') data
Megias et al., Phys.Rev. D94 (2016) 013012

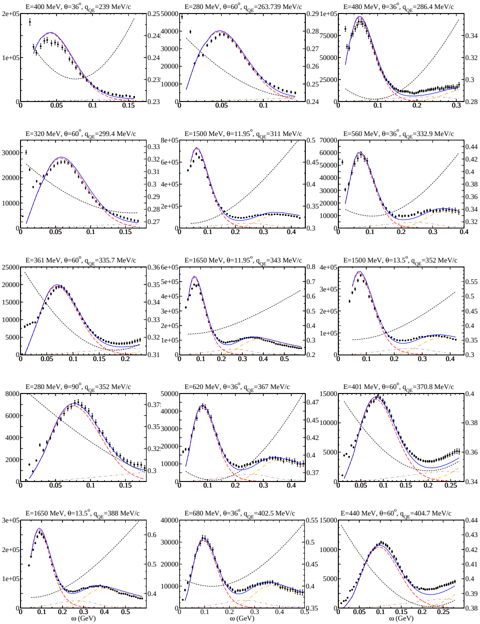
E=400 MeV, θ=36°, q_QE=239 MeV/c
E=280 MeV, θ=60°, q_QE=263.739 MeV/c
E=480 MeV, θ=36°, q_QE=286.4 MeV/c
E=320 MeV, θ=60°, q_QE=299.4 MeV/c
E=1500 MeV, θ=11.95°, q_QE=311 MeV/c
E=560 MeV, θ=36°, q_QE=332.9 MeV/c
E=361 MeV, θ=60°, q_QE=335.7 MeV/c
E=1650 MeV, θ=11.95°, q_QE=343 MeV/c
E=1500 MeV, θ=13.5°, q_QE=352 MeV/c
E=280 MeV, θ=90°, q_QE=352 MeV/c
E=620 MeV, θ=36°, q_QE=367 MeV/c
E=401 MeV, θ=60°, q_QE=370.8 MeV/c
E=1650 MeV, θ=13.5°, q_QE=388 MeV/c
E=680 MeV, θ=36°, q_QE=402.5 MeV/c
E=440 MeV, θ=60°, q_QE=404.7 MeV/c
ω (GeV)

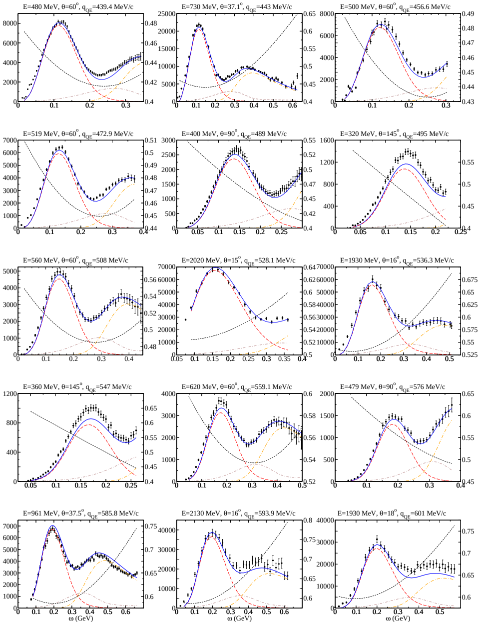
E=480 MeV, θ=60°, q_QE=439.4 MeV/c
E=730 MeV, θ=37.1°, q_QE=443 MeV/c
E=500 MeV, θ=60°, q_QE=456.6 MeV/c
E=519 MeV, θ=60°, q_QE=472.9 MeV/c
E=400 MeV, θ=90°, q_QE=489 MeV/c
E=320 MeV, θ=145°, q_QE=495 MeV/c
E=560 MeV, θ=60°, q_QE=508 MeV/c
E=2020 MeV, θ=15°, q_QE=528.1 MeV/c
E=1930 MeV, θ=16°, q_QE=536.3 MeV/c
E=360 MeV, θ=145°, q_QE=547 MeV/c
E=620 MeV, θ=60°, q_QE=559.1 MeV/c
E=479 MeV, θ=90°, q_QE=576 MeV/c
E=961 MeV, θ=37.5°, q_QE=585.8 MeV/c
E=2130 MeV, θ=16°, q_QE=593.9 MeV/c
E=1930 MeV, θ=18°, q_QE=601 MeV/c
ω (GeV)

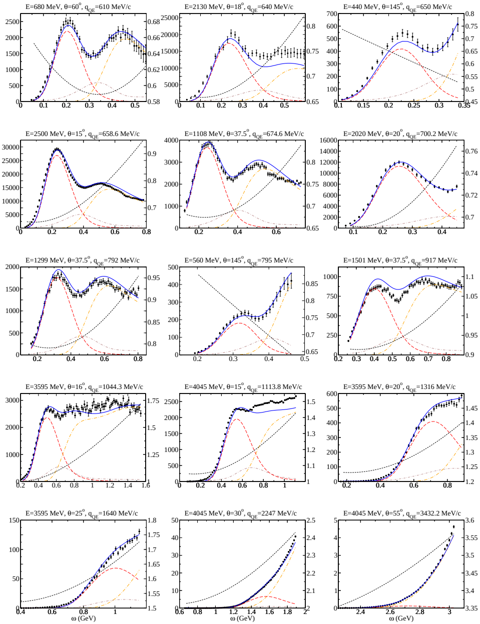
E=680 MeV, θ=60°, q_{QE}=610 MeV/c
E=2130 MeV, θ=18°, q_{QE}=640 MeV/c
E=440 MeV, θ=145°, q_{QE}=650 MeV/c
E=2500 MeV, θ=15°, q_{QE}=658.6 MeV/c
E=1108 MeV, θ=37.5°, q_{QE}=674.6 MeV/c
E=2020 MeV, θ=20°, q_{QE}=700.2 MeV/c
E=1299 MeV, θ=37.5°, q_{QE}=792 MeV/c
E=560 MeV, θ=145°, q_{QE}=795 MeV/c
E=1501 MeV, θ=37.5°, q_{QE}=917 MeV/c
E=3595 MeV, θ=16°, q_{QE}=1044.3 MeV/c
E=4045 MeV, θ=15°, q_{QE}=1113.8 MeV/c
E=3595 MeV, θ=20°, q_{QE}=1316 MeV/c
E=3595 MeV, θ=25°, q_{QE}=1640 MeV/c
E=4045 MeV, θ=30°, q_{QE}=2247 MeV/c
E=4045 MeV, θ=55°, q_{QE}=3432.2 MeV/c
ω (GeV)
ω (GeV)
ω (GeV)

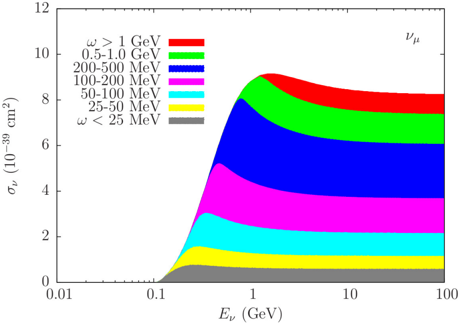
$\omega > 1$ GeV
0.5-1.0 GeV
200-500 MeV
100-200 MeV
50-100 MeV
25-50 MeV
$\omega < 25$ MeV
ν_μ
σ_ν (10^{-39} cm^2)
E_ν (GeV)
0
2
4
6
8
10
12
0.01
0.1
1
10
100

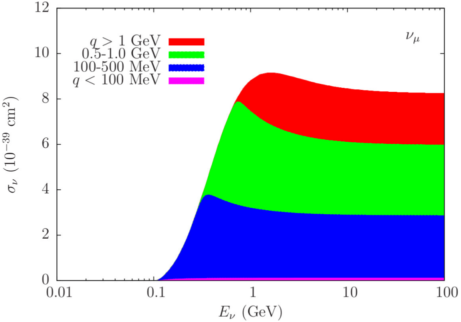
$q > 1$ GeV
0.5-1.0 GeV
100-500 MeV
$q < 100$ MeV
ν_μ
σ_ν (10^{-39} cm^2)
E_ν (GeV)
0
2
4
6
8
10
12
0.01
0.1
1
10
100

MiniBooNE and NOMAD CCQE

$\nu_\mu - C$

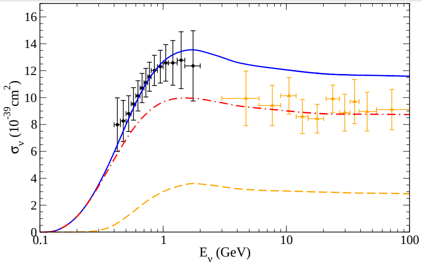

$\bar{\nu}_\mu - C$

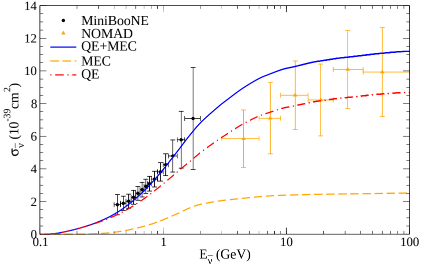

SciBooNE inclusive ν_μ-C and $\bar{\nu}_\mu$-CH

Megias *et al.*, PRD 94, 093004 (2016)

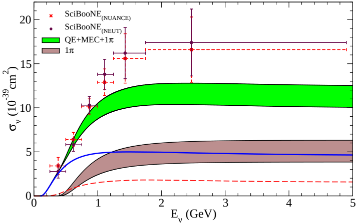

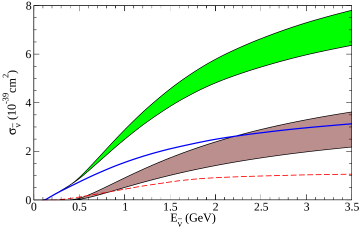

On the importance of relativistic effects

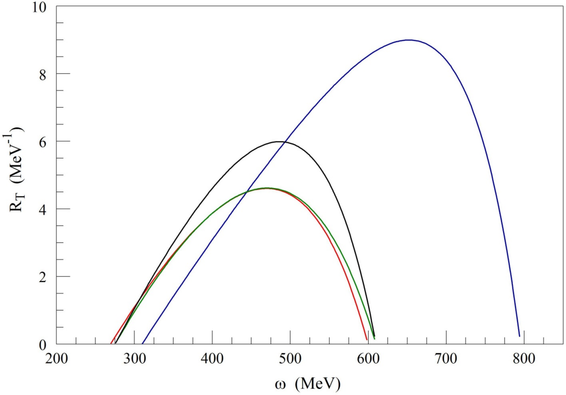

- Red: exact relativistic RFG
- Blue: exact non-relativistic NRFG
- Black: NRFG with relativistic kinematics only
- Green: NRFG with relativistic kinematics and current operators